Journal of Building Pathology and Rehabilitation (2020) 5:1
https://doi.org/10.1007/s41024-019-0067-3

RESEARCH ARTICLE

Corrosion assessment and control techniques for reinforced concrete structures: a review

Md Daniyal[1] · **Sabih Akhtar**[1]

Received: 14 December 2018 / Accepted: 12 November 2019 / Published online: 18 November 2019

Abstract
Steel corrosion is the main source of damage and early failure of reinforcement concrete structures that in turns create huge economical loss and creating environmental problems. In the past, several corrosion assessment techniques such as potential measurement, gravimetric weight loss measurement, electrical resistivity measurement, sensors and electrochemical methods for instance potentiodynamic polarization, linear polarization resistance, galvanostatic pulse, and electrochemical impedance have been developed to detect corrosion condition of steel in concrete. Though the potential measurement, resistivity measurement and sensors can only provide the qualitative information about the steel corrosion. The weight loss measurement is an efficient technique for corrosion rate measurement of steel, but it is destructive and requires long exposure times. The electrochemical techniques are non-destructive in nature and are used to determine corrosion rate of steel in laboratory as well as field studies. However each of these methods possesses certain advantages and limitations, therefore a combination of these techniques is recommended to use to obtain the corrosion condition of steel. As far as corrosion control techniques for steel reinforced concrete are concerned, several methods such as cathodic protection, electrochemical chloride extraction, surface treatments of the steel, surface treatment of concrete, utilization of mineral admixtures and chemical corrosion inhibitors have been developed in the past. Each of these methods offers some advantages and disadvantages. Thus, more researches are required to develop such methods of corrosion protection of steel that are economical, durable, environment-friendly and do not cause any adverse effect on the structural performance of concrete and steel.

Keywords Steel corrosion · Economical loss · Environmental problems · Corrosion assessment techniques · Corrosion control techniques

1 Introduction

Prior to the invention of cement, mortars were made by mixing water, sand and slaked lime [1]. John Smeaton discovered hydraulic lime mortars in 1754 [2]. A British mason named Joseph discovered the cement in 1824 and filed the first patent on Portland cement [3]. However, the objects prepared with the use of Portland cement were extremely brittle and incapable to tolerate shocks. Joseph Monier, a French gardener in 1867 made flowerpots with embedded iron nails and consequently observed a remarkable enhancement in the durability of his pots. Afterward, efficient scientific developments in concrete manufacture took place. In 1911, American Society for Testing and Materials (ASTM) formulated a detailed specification for the utilization of steel in concrete [4]. Subsequently, various developments ensued in designing the steel reinforcement bars in order to produce stronger and durable concrete structures. Consequently, the steel-reinforced concrete became the most widely used structural material in the world because of its economical, strength and durability properties. Steel-reinforced concrete structures were viewed as maintenance-free and unlimited service life until the mid-1970s. Conversely, since then, several durability related problems have emerged, such as alkali-silica reactions, sulphate attacks and corrosion of steel reinforcement. Among all durability related problems in steel-reinforced concrete structures, corrosion of steel reinforcement has been recognized as the main source of deterioration [5].

Generally, the corrosion affects our daily lives directly as well as indirectly. In direct, it shortens the useful service

✉ Md Daniyal
daniyalzhcet@gmail.com

[1] Department of Civil Engineering, Aligarh Muslim University, Aligarh, India

life of our goods. In indirect, the manufacturer and provider of goods and services incur costs of corrosion from the clients. In particular, the corrosion of reinforcing steel bar in concrete results the collapse of bridges, failure of a part of highways, damage to buildings, and parking structures, etc. consequently endangers public safety and requires considerable repair costs. For instance, the unexpected collapse of the Silver Bridge over the Ohio River at Point Pleasant due to corrosion fatigue in 1967 resulted in deaths of 46 people and cost millions of dollars [6]. Therefore, in order to estimate the cost of corrosion in the United States (US), a study entitled "Corrosion Costs and Preventive Strategies in the United States" was conducted with the help of Federal Highway Administration (FHWA) and National Association of Corrosion Engineers (NACE) International, from 1999 to 2001 by CC Technologies Laboratories. This investigation estimated the average direct cost of corrosion of $8.3 billion per year for highway bridges alone and the total corrosion cost of US industries was estimated to $276 billion annually, which is approximately equal to 3.1% of the US Gross Domestic Product (GDP) [7]. In 2014, a study entitled "International Measures of Prevention, Application, and Economic of Corrosion Technologies (IMPACT)" was initiated by NACE International and conducted by Det Norske Veritas (DNV), Germanischer Lloyd (GL), and American Productivity and Quality Center (APQC) and its industry and technology partners worldwide. From this study, the cost of corrosion at the global level is estimated to be $2.5 trillion per year, which is about 3.4% of the global GDP in 2013 [8]. Hence, from the safety and economical perspective, the corrosion of steel reinforcement is very serious problem that can affect the sustainability of the steel-reinforced concrete structures directly. Numerous studies have been conducted worldwide in order to extend service life of steel reinforced concrete structures; regardless of this, several aspects are still not well known, and there is the requirement to incorporate present facts into practical field.

In this paper, an attempt has been made to review the studies pertaining to corrosion of steel reinforced concrete conducted by various investigators. The paper is organized in two major thematic sections. In the first section, an overview of various corrosion monitoring techniques for steel reinforced concrete has been undertaken. The second section includes studies related to the different corrosion control methods for steel reinforced concrete.

2 Corrosion assessment techniques

The maintenance and repair of steel reinforced concrete structures for their safety needs effective monitoring and inspection methods for evaluating the corrosion of steel reinforcement. These methods need to be able to identify any probable durability problems within structures before they become severe. Since the corrosion of steel reinforcement occurs through electrochemical reactions involving charge (electrons) transfer via concrete pore solution (electrolyte), electrochemical methods are appropriate to study the corrosion processes. In this section, some electrochemical and non-destructive techniques commonly used for monitoring the corrosion of steel in concrete structures have been discussed. Further, a destructive technique viz. the gravimetric weight loss method and corrosion monitoring using sensors have been reviewed.

2.1 Open circuit potential measurement

The basic principle involved in this method is the measurement of corrosion potential (also called half-cell potential or open circuit potential) of steel reinforcement with respect to a standard reference electrode (RE) such as copper/copper sulphate electrode (CSE), silver/silver chloride electrode (SSCE), standard hydrogen electrode (SHE) and Saturated Calomel Electrode (SCE). The reference electrode has a predetermined potential. For example, the SCE has a potential of + 242 mV vs. the SHE (assumed potential of 0.0 V) at room temperature. The schematic diagram for open circuit potential (E_{OC}) measurement is shown in Fig. 1 [9]. In accordance with ASTM C 876, the probable corrosion conditions of steel reinforcement related with E_{OC} values is presented in Table 1 [10].

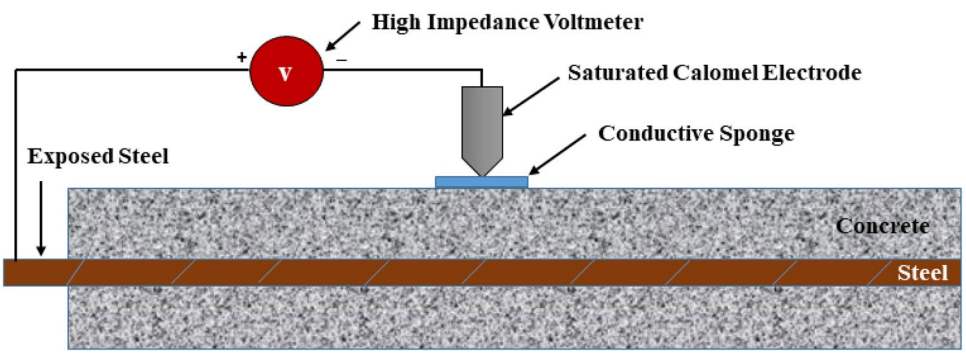

Fig. 1 Illustration of E_{OC} measurement technique [9]

Table 1 Corrosion risk of steel reinforcement associated with E_{OC} values [10]

E_{OC} values				Corrosion risk
(mV vs. CSE)	(mV vs. SSCE)	(mV vs. SHE)	(mV vs. SCE)	
< − 500	< − 406	< − 184	< − 426	Severe
< − 350	< − 256	< − 34	< − 276	High
− 350 to − 200	− 106 to − 256	+ 116 to − 34	− 126 to − 276	Intermediate
> − 200	> − 106	> + 116	> − 126	Low

The open circuit potential (E_{OC}) of a steel is a measure of its tendency to corrode. However, these E_{OC} values are not sufficient criterion, as they are affected by many factors, such as polarization by partial diffusion of O_2, porosity of concrete and the existence of resistive layers. Therefore, it is commonly believed that E_{OC} measurement must be complemented by other techniques [11]. This technique is very useful in identifying the anodic and cathodic locations in steel–concrete structures by drawing potential map. Numerous investigators have studied the effectiveness of this method and got advantageous outcomes [12–14]. However, E_{OC} values can provide information for degree of corrosion risk only and cannot specify the corrosion rate [15].

2.2 Surface potential measurement

This is another useful non-destructive method to identify the condition of steel embedded in concrete. In this method, two reference electrodes are used as shown in Fig. 2 [9]. One electrode is kept fixed (called fixed electrode), the other electrode (called movable electrode) is moved along the structure on the nodal points. When movable electrode is placed at the nodal points, the potential is measured against the fixed electrode by means of a high impedance voltmeter. A more positive potential value signifies anodic region where corrosion is possible. The higher the potential difference between anodic and cathodic zones higher is the possibility of corrosion. Therefore, surface potential measurement is used for detecting anodic and cathodic areas in steel–concrete structures and ultimately identifying the possibility of corrosion of steel in concrete [9].

Although potential measurement techniques (open circuit potential and surface potential measurements) have been used extensively, some of their limitations has described as follows:

(a) The measured potential difference between the reference electrode and the steel in concrete depends on the corrosion condition of the steel and on the type of reference electrode used [16].
(b) A simple comparison of the measured potential values with the ASTM recommendations on probability of steel rebar corrosion could not be useful. This is because of the fact that a more negative value of potential, which is usually considered to specify a greater possibility of corrosion, may not be valid always as several factors can change the potential values towards more negative or positive values [17].
(c) While performing the potential measurements, potential values should be interpreted according to the resistivity of the steel reinforced concrete system. Otherwise, the outcomes can be misrepresentative for the same degree of corrosion. Thus, one can get different potential readings at the surface of concrete, corresponding to different values of resistivity, and consequently have more than one probability for the same condition of corrosion [18].

On account of the above limitations, the use of potential measurements is considered as the first methodology for detection of corrosion, and thus requires to be complemented with other non-destructive methods for advance diagnosis.

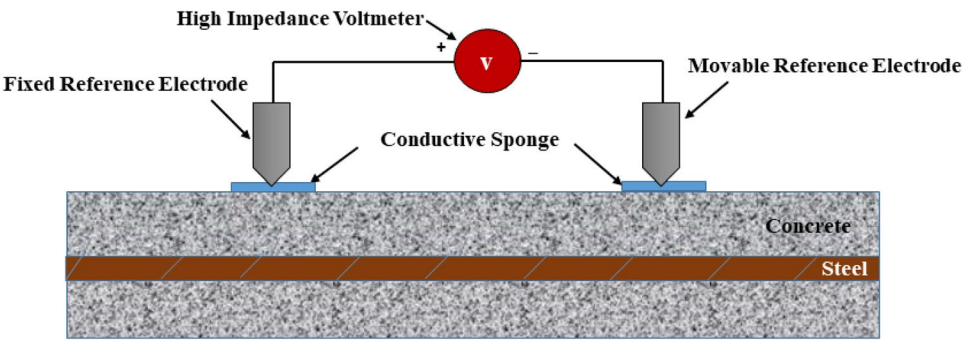

Fig. 2 Schematic diagram of surface potential measurement [9]

2.3 Potentiodynamic and cyclic polarization

The recent theory of electrochemical corrosion is based on electrode kinetics. The corroding system wherein a single anodic reaction and a single cathodic reaction take place on a single electrode surface, the relationship of the current as a function of potential can be written as Eq. (1). This equation is derived by the application of the mixed potential theory and Butler-Volmer equation [19–21]:

$$i = i_{corr}\left[\exp\left\{\frac{2.303(E - E_{corr})}{\beta_a}\right\} - \exp\left\{\frac{-2.303(E - E_{corr})}{\beta_c}\right\}\right] \quad (1)$$

where, i = external current density (A/cm^2), E = potential applied to polarize the corroding system (V), E_{corr} = corrosion potential (V), i_{corr} = corrosion current density (A/cm^2), β_a = anodic Tafel constant (V/decade), β_c = cathodic Tafel constant (V/decade). However, when E is far away from E_{corr}, then the Eq. (2) gives the Tafel equation [22]:

$$E = a \pm b \log |i| \quad (2)$$

where, a = a constant and b = β_a or β_c

The Eq. (2) shows that the variation of the logarithm of the external current density with the potential is linear at high overpotential. The i_{corr} can be calculated by extrapolating the anodic and cathodic straight lines of E vs. log |i| plot at the $E_{corr.}$ Moreover, the E vs. log |i| plot and various corrosion kinetic parameters can be determined easily by conducting potentiodynamic and cyclic polarization test using inbuilt software provided by the potentiostat manufacturer. A potentiostat is a specifically designed instrument that measures the potential/current characteristics of an electrochemical (electrode/solution) interface [23].

In order to perform the potentiodynamic or the cyclic polarization scan, three electrodes, electrolyte (testing solution) and a potentiostat are required. The electrodes include a working electrode (the test sample itself), a counter or auxiliary electrode (used to transport the current to the working electrode and to close the electrical circuit) and a reference electrode (used to measure the potential difference). In order to conduct the scan, these electrodes are to be immersed in the electrolyte and attached to the potentiostat [13, 14]. Moreover, the potentiostat is a device that is used to apply potential and record the induced current or vice versa. More explicitly, both controlled-current (Galvanostatic) and controlled-potential (Potentiostatic) polarization can be applied. The term 'polarization' means the perturbation of the potential of a sample in electrolyte from its open circuit potential (E_{oc}). This can be done by two ways, i.e. when the polarization is accomplished galvanostatically, potential is measured and when it is achieved potentiostatically, current is measured. However, the potentiostatic method is much more common than galvanostatic method. The response (i.e., resulting current) of the sample is measured as it is polarized. The response is used to develop a model of the sample's corrosion behaviour [9].

The potentiodynamic polarization is used to study the corrosion behaviour and to calculate the different corrosion parameters such as corrosion current density (i_{corr}) of a corroding system in a certain environments. In a usual potentiodynamic scan, the potential (E) is swept over a fixed range by potentiostat and the induced current is recorded as a function of potential. The graphical output of a potentiodynamic scan is referred to as Tafel plot (named after Swiss chemist Julius Tafel), which is a plot of the potential (E) versus the logarithm of the current density (log |i|). In order to perform several tests on one sample (i.e., non-destructive test) the scan range should be within the Tafel region. Applying excessive anodic potential will force the system to corrode (i.e. destructive testing) [1, 15].

The analysis of Tafel plots is performed by corrosion test software (such as Gamry Instruments, ACM Instruments etc.). The corrosion parameters (such as E_{corr}, i_{corr}, β_a, and β_c) are determined by intersecting the open circuit potential (E_{OC}) and the extrapolation of the linear portions of logarithmic current plot as shown in Fig. 3 [12, 16]. Knowing the corrosion current density (i_{corr}) the corrosion rate (CR) can be calculated using Eq. (3) [28]. Though, this can also be estimated by corrosion test software provided by potentiostat manufacturer.

$$CR = \frac{i_{corr} \times K \times (EW)}{d \times A} \quad (3)$$

where, EW (equivalent weight) = Theoretical mass of metal that will be lost from the sample after one Faraday of anodic charge has been passed (EW = atomic weight/valence), i_{corr} = corrosion current density (mA/cm^2), K = a constant that defines the units for the corrosion rate (for CR in mm/

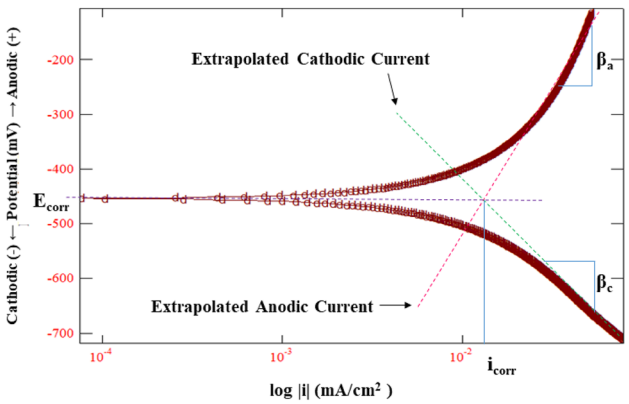

Fig. 3 Typical potentiodynamic polarization curve [12]

year (mmpy), K = 3272; and CR in milli-inches/year (mpy), $K = 1.288 \times 10^5$), d = density (g/cm^3), A = specimen area (cm^2)

The cyclic polarization test is used primarily to study the pitting corrosion behaviour of metal in a certain environmental condition. Therefore, in this test, sufficiently high anodic potential is to be applied to ensure initiation of pitting corrosion. As soon as the scan is reached at anodic potential limit E_{rev} (reverse potential), the path of the scan is reversed on the way to the cathodic direction until the ultimate predetermined potential is reached. The potential at the scan plot in which the induced current sharply increases is called the pitting potential (E_{pit}). The potential on the reverse scan where the loop closes is called the protection potential (E_{prot}), below which no pitting corrosion is likely to take place. If the Eprot is more positive than the Epit, then pitting will not occur. Though, pitting could occur if the E_{prot} is more negative than the E_{pit}. In general, the extent of the hysteresis loop indicates the degree of pitting tendency. The greater the loop size, the higher the pitting tendency and vice versa. Figure 4 shows a detailed cyclic polarization scan curve [29–31].

In this technique, the conductivity of the electrolyte (environment) plays very important role. The resistance of electrolyte lowers the potential between the reference electrode and working electrode and can cause errors in the readings. This aspect has significant effects on the interpretation, and should be compensated. Therefore, this factor should be considered while performing the potentiodynamic cyclic polarization measurement.

2.4 Linear polarization resistance

The linear polarization resistance (LPR) technique can be applied in both field and lab measurements. It is a direct current (DC) technique, first introduced by Stern and Geary in 1957 [32–34]. In this technique, a small polarization perturbation (between 10 and 30 mV) is applied about E_{OC} of metal using a potentiostat and the resulting induced current is recorded. Although, the corrosion is an electrochemical process and does not comply with the Ohm's law (i.e. linear relationship between current and potential). However, it has been found that Ohm's law will be nearly true if polarization potential is very small [35]. Since in this method the applied potential is small, therefore the current response will be linear. A typical potential and current density (obtained by dividing the current response by known surface area of working electrode) plot is shown in Fig. 5 [25, 26].

The slope of the potential–current density plot near E_{OC} is defined as linear polarization resistance (R_p) [38]. In case of steel reinforced concrete system, the R_p includes the concrete resistance (R_C) and charge transfer resistance (R_{ct}). Thus, linear polarization can be estimated as follows [28, 29]:

$$R_p = \frac{\Delta E}{\Delta i} = R_C + R_{ct} \tag{4}$$

The corrosion current density is then determined using the Stern–Geary formula:

$$i_{corr} = \frac{B}{R_p} \tag{5}$$

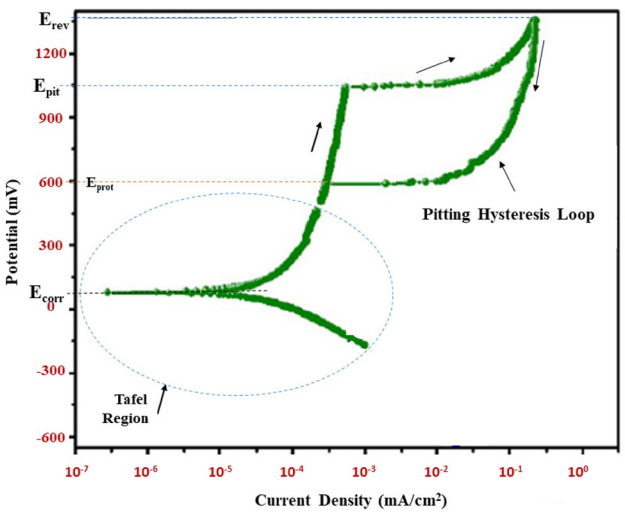

Fig. 4 Typical cyclic polarization curve [29]

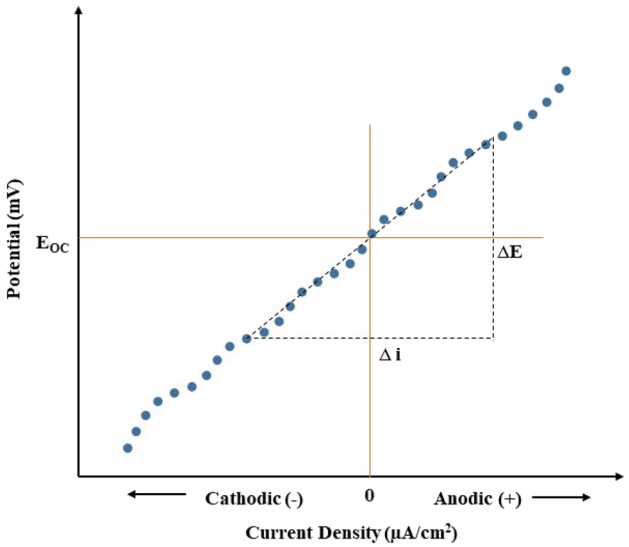

Fig. 5 Typical linear polarization plot [25]

where, i_{corr} is the corrosion current density (μA/cm^2), Rp is the polarization resistance (kΩ cm^2) and B can be calculated by the following relationship:

$$B = \frac{\beta_a \times \beta_c}{2.3(\beta_a + \beta_c)} \quad (6)$$

where, β_a and β_c are the anodic and cathodic Tafel constants in mV/decade, respectively.

The Tafel constants are usually obtained from Tafel plot (by polarizing the steel to ± 250 mV of the E_{OC}). However, in the absence of necessary data on β_a and β_c, B = 26 mV (for actively corroding steel in concrete) and B = 52 mV (for steel in passive situation) is used to compute the corrosion current density [41]. Moreover, the corrosion current density is inversely proportional to the linear polarization resistance. Hence, high polarization resistance value indicates low corrosion rate, and vice versa.

In order to carry out the linear polarization resistance investigation, similar to the potentiodynamic and cyclic polarization test, three electrodes are to be connected to a potentiostat. These are the working electrode (corroding metal), the auxiliary (counter) electrode and the reference electrode [35].

Several investigation has used a corrosion current density limit of 0.1–0.2 μA/cm^2 to distinguish between passive and active corrosion state of steel embedded in concrete [31, 32]. In addition, many study reported different limits (in terms of corrosion current density, linear polarization resistance and corrosion penetration rate) in order to separate the different degree of corrosion risk associated with steel reinforcement, as listed in Table 2 [1, 24].

Even with complexities, the LPR measurements method pose several complications in high resistivity media, for instance those encountered in huge steel reinforced concrete structures. Noteworthy amongst such complications has been described as follows, which may even render the in situ measurement extremely inaccurate.

a. The resistance of concrete between the steel rebar (working electrode) and the reference electrode is very high. This offers a potential drop generally referred to as an Ohmic drop and that must be either compensated externally or removed mathematically.
b. The counter electrode being smaller compared to the sample, the distribution of the applied electrical signal for polarisation of the steel rebar is non-uniform throughout the cross-section of the sample.

Table 2 Typical corrosion criteria of steel embedded in concrete [1, 24]

Corrosion condition	Polarization resistance (kΩ cm^2)	Current density (μA/cm^2)	Corrosion penetration rate (μm/year)
Very high	2.5–0.25	10–100	100–1000
High	25–2.5	1–10	10–100
Low/moderate	250–25	0.1–1	1–10
Passive	> 250	< 0.1	< 1

2.5 Electrochemical impedance spectroscopy

This technique is also known as alternating current (AC) impedance spectroscopy, because in this method, an AC excitation potential with variable frequencies is applied to the specimen (working electrode) and the induced AC current response is measured. The AC excitation potential should be very low (usually between 5 and 20 mV) in order to retain in the linear zone and to perform non-destructive testing. In the linear zone, the AC current (induced) will have the different amplitude and identical frequency as the applied AC excitation potential, but with a phase difference. The impedance (that includes real and imaginary parts) is the ratio of AC potential to AC current, and can be calculated from the following relationships [33, 34]:

$$Z = \frac{E(t)}{I(t)} = \frac{E_0 \mathrm{Cos}(\omega t)}{I_0 \mathrm{Cos}(\omega t - \Phi)} = Z_0 \frac{\mathrm{Cos}(\omega t)}{\mathrm{Cos}(\omega t - \Phi)} \quad (7)$$

$$Z = Z_0 \left[\exp(j \cdot \Phi)\right] = Z_0(\mathrm{Cos}\Phi + j \cdot \mathrm{Sin}\Phi) = Z' + jZ'' \quad (8)$$

where, Z = complex impedance, E (t) = potential at time t, I (t) = current at time t, E_0 = potential amplitude, I_0 = current amplitude, ω = radial frequency, ϕ = phase difference between potential and current, Z_0 = magnitude of complex impedance, $j = \sqrt{-1}$

The real part (Z′) and imaginary part (Z″) of the impedance (Z) represent resistive and capacitive/inductive terms respectively. The graph of Z' on the abscissa and Z" on the ordinate, measured at various frequencies (usually between 100 kHz and 10 mHz) is called as impedance spectrum or impedance graph or Nyquist plot. In order to determine various parameters (such as solution resistance, charge transfer resistance and double layer capacitance), the Nyquist plot has to be fitted and modelled with an equivalent electrical circuit that indicate the electrochemical processes at the specimen. Particularly in the steel reinforced concrete specimens, various equivalent circuits have been suggested due to complex nature of the steel–concrete interface. The simplest electrochemical equivalent circuit known as Randels circuit shown in Fig. 6 can be used for modelling the typical Nyquist plot shown in Fig. 7 [46–48].

The equivalent circuit comprises of a resistance R_c linked in series to a loop that contains a different resistance R_{ct} and a capacitance C_{dl} joined in parallel. The R_c

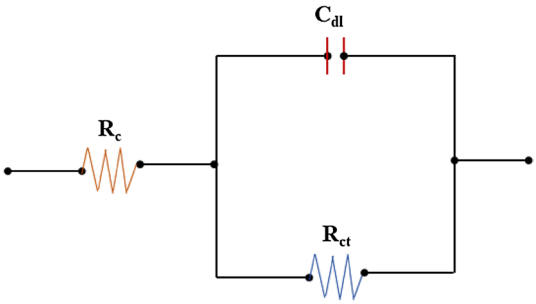

Fig. 6 Rendles electrical equivalent circuit for steel reinforcement [46–48]

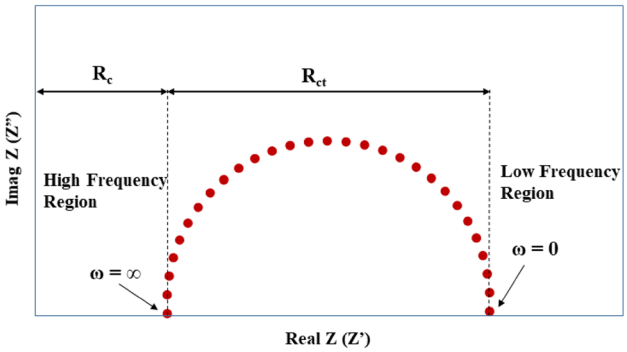

Fig. 7 Typical Nyquist plot for steel reinforcement [46–48]

indicates the concrete pore electrolyte resistance or concrete cover resistance. The R_{ct} is the charge transfer resistance at the surface of steel that represents the ease with which the charged ions can leave the steel surface and reach into the electrolyte (i.e. metal dissolution resistance). The C_{dl} is a double layer capacitor, which refers to the development of two layers on the steel/electrolyte interface. The first layer is formed due to the attraction of molecules towards the steel surface anions (free electrons). The second layer is formed due to the attraction of molecules towards cations in the pore solution. Moreover, R_{ct} and C_{dl} both resembles to the ionic resistance of the corrosion products film developed on the steel surface. These terms are illustrated in Fig. 8 [24, 38].

From the Rendles equivalent circuit, the equivalent impedance (Z) of the Nyquist plot is represented as follows [39]:

$$Z = R_C + \frac{R_{ct}}{1 + j\omega C_{dl} R_{ct}} \quad (9)$$

where, R_c = concrete resistance, R_{ct} = charge transfer resistance, $j = \sqrt{-1}$, $\omega = 2\pi f$, C_{dl} = double layer capacitance

When, $\omega \to 0$ (i.e. at low frequency), the circuit turn into DC circuit and therefore

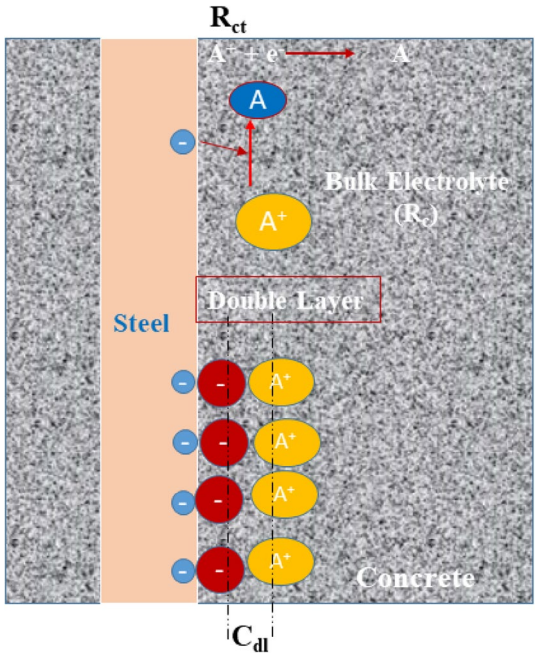

Fig. 8 Impedance components in steel concrete interface [38]

$$Z = R_c + R_{ct} = R_p$$

When, $\omega \to \infty$ (i.e. at high frequency, AC circuit), $Z = R_c$

The difference of DC and AC impedance gives the true polarization resistance as:

True polarization resistance $= (R_c + R_{ct}) - R_c = R_{ct}$

Accordingly, the diameter of the extrapolated semicircle in the Nyquist plot indicates the charge transfer resistance (R_{ct}), which is equivalent to the true polarization resistance. Thus, if the diameter of the semicircle will be large, then polarization resistance will be high and corrosion rate will be low, and vice versa [45].

Owing to sophistication of the measurement, this method is more extensively used in laboratory investigations rather than in field. It needs more time to perform and its interpretation is also difficult. However, nowadays it used as a research tool to recognize the behaviour and mechanism of the concrete/steel interface and to reveal facts of the steel rebar corrosion kinetics [50].

2.6 Galvanostatic pulse

This is a rapid and non-destructive polarisation method. It was introduced in 1988 for field application [51]. In this technique, galvanostatically a short-time anodic current pulse (usually 10–100 μA with pulse duration of 5–30 s) is applied between the steel reinforcement and auxiliary (counter) electrode placed on the surface of concrete. The reference electrode is commonly placed in the centre of the auxiliary electrode. The steel is polarised anodically and the

resulting electrochemical potential response of the steel is recorded using a reference electrode as a function of polarisation time. The characteristic electrochemical potential response of corroding steel is shown in Fig. 9 [52].

When the current pulse, I_{app}, is applied to the steel reinforcement, then the polarisation of the steel at time t, E_t, can be written as follows [53–55]:

$$E_t = I_{app}\left[R_p\left\{1 - e^{\left(\frac{-t}{R_p C_{dl}}\right)}\right\} + R_{tc}\right] \quad (10)$$

where, R_p = polarisation resistance, C_{dl} = double layer capacitance, R_c = concrete cover resistance, R_p and C_{dl} can be determined by transforming the Eq. (10) into linear form as [53, 54]:

$$\log\left(E_{max} - E_t\right) = \log\left(I_{app} \times R_p\right) - \left(\frac{t}{R_p C_{dl}}\right) \quad (11)$$

where, E_{max} = Final steady state potential

A typical plot of Eq. (11) is shown in Fig. 10 [53]. If the straight line passing through the data points is extrapolated to time (t) = 0, then the intercept at ordinate will give $\log(I_{app} \times R_p)$ and slope of the straight line will yield $1/(R_p \times C_{dl})$. The residual overpotential analogous to $(I_{app} \times R_c)$ i.e. potential drop across the cover concrete. After finding the Rp by applying above technique, the corrosion current density (i_{corr}) can be determined from Sterne Geary formula (Eq. 5) [46].

2.7 Electrical resistivity measurement

The durability characteristics of concrete can be assessed by determining its electrical resistivity. Various investigations have given the correlation between electrical resistivity of concrete and corrosion of steel reinforcement [56–58].

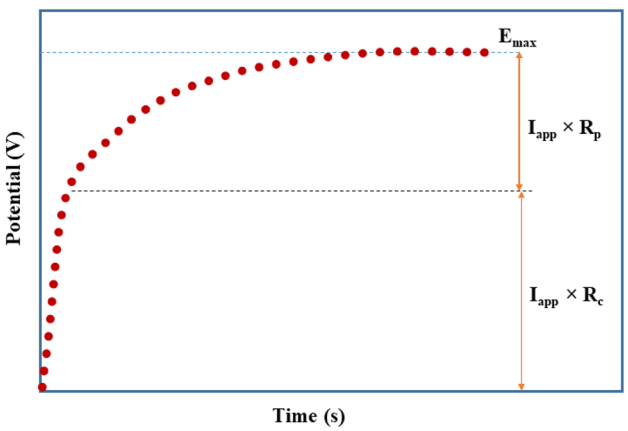

Fig. 9 Electrochemical potential response of corroding steel [52]

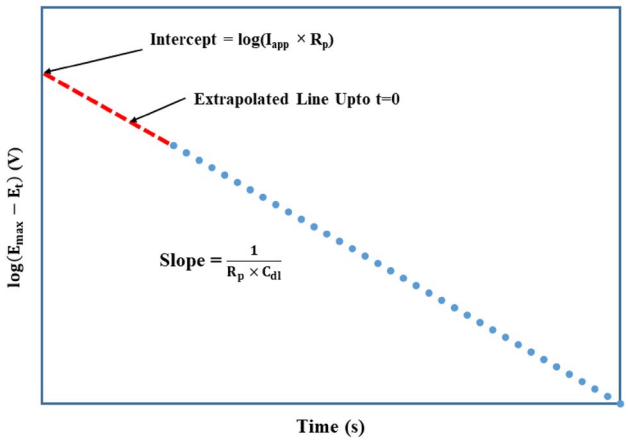

Fig. 10 A typical plot of Eq. (11) [53]

Several researchers have tried to made the relationship between the concrete resistivity and the different concrete properties such as water/cement ratio, cement content, coarse aggregate content, age, diffusion coefficient of chloride and porosity [59–61].

The electrical resistivity of concrete is commonly measured using four-probe technique. F. Wenner firstly introduced this technique in order to evaluate the soil resistivity [62]. After that, this method was widely applied for the concrete resistivity measurement in the lab as well as field. The Fig. 11 illustrates principle involved in the Wenner four-probe electrical resistivity measurement technique [63]. In this method, four equally spaced electrodes (probes) are used to measure the concrete resistivity. A small AC current (I) is applied between the outermost probes whereas potential difference (V) between the inner probes is recorded. Then, the surface resistivity of concrete is determined from the Eq. (12) [64].

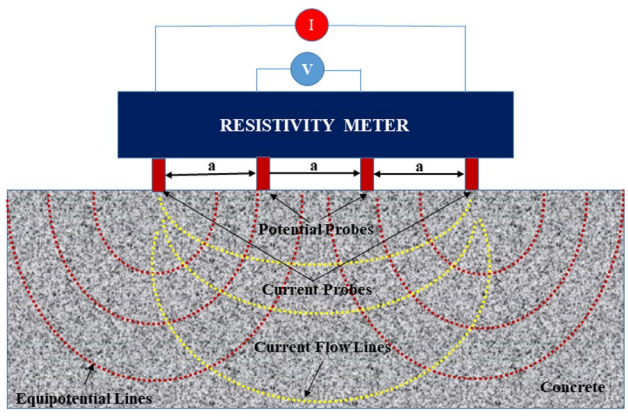

Fig. 11 Illustrations of the Wenner four-probe resistivity measurement [53]

$$\rho = ka\frac{V}{I} \tag{12}$$

where; a = distance between the probes, k = geometry factor = 2π (for semi-infinite body such as concrete slabs)

However, the value of k is different for small cubic or cylindrical specimens used in laboratory testing condition. The AASTHO TP 95-11 Standard specified the typical value of 'a = 38 mm' and 'AC frequency = 13 Hz' in order to conduct the concrete surface electrical resistivity measurement [65].

Moreover, it is extensively recognized that resistivity of concrete can be easily determined, particularly in the field, compared to other corrosion parameters such as corrosion rate. Various investigators as presented in Table 3 have developed the correlation between the resistivity of concrete and steel reinforcement corrosion risk [65].

The variations in the results show that the concrete resistivity could not be used with full confidence as an indicator for corrosion activity in steel reinforcement and need more investigations. Furthermore, various factors that might affect the results of resistivity measurement of concrete include water/cement ratio, microstructural properties of concrete, aging, existence of steel reinforcement, geometrical constraints, surface contact of probes, spacing between probes, temperature, and moisture content [63].

2.8 Gravimetric weight loss measurement

This is the most commonly used destructive technique for estimating the corrosion rate of steel reinforcement [59, 60]. The detailed guideline for the preparation of test specimens and evaluation of corrosion rate by means of gravimetric weight loss measurement has been specified in ASTM G1-03 [73]. In order to carry out this test, firstly, the steel is to be immersed in the Clark solution (1L of HCl + 50 g of $SnCl_2$ + 20 g of Sb_2O_3) for 40 s, then, degreased with acetone, rinsed with distilled water and dried in air. Thereafter, the initial weight of the steel is taken using an electronic weighing balance with 0.1 mg precision before embedding in concrete. After a specified period of exposure in the corrosive medium, the steel is taken out by splitting the concrete specimens. After that, the corroded steel is to be cleaned by the above procedure and finally, weighed again. The obtained weight loss value is to be used to estimate the corrosion rate (CR) by the following relationship [74]:

$$CR = \frac{K \times \Delta W}{A \times T \times \rho} \tag{13}$$

where, ΔW = weight loss (g), A = exposed surface area (cm^2), T = Time of exposure (hours), K = unit conversion constant = 8.76×10^4 (for mm/year) = 534 (for mils/year), ρ = density (g/cm^3)

This is the most accurate and precise technique for determining the corrosion rate of steel reinforced concrete system because the testing is easy to replicate. This is comparatively simple method that reduces the tendency to lead methodical errors. The sensitivity of mass loss measurements is limited because mass can be measured easily only to about 0.1 mg, therefore this key issue must be considered while using this method. Further, this technique is destructive and generally performed after long exposure periods, consequently provide an average corrosion rate.

Table 3 Relationship between concrete resistivity and corrosion risk [65]

Corrosion risk in terms of concrete resistivity (kΩ cm)			References
High	Moderate	Low	
< 5	5–12	> 12	[56]
< 6.5	6.5–8.5	> 8.5	[57]
< 7	7–30	> 30–40	[58]
< 10	10–30	> 30	[66]
< 20	20–100	> 100	[67]
< 10	10–100	> 100–200	[68]
< 5	5–20	> 20	[69]
< 8	8–12	> 12	[70]

2.9 Corrosion monitoring using sensors

The latest advances in the field of smart materials and systems have escorted novel openings for structural health monitoring and non-destructive evaluation. Smart materials, for instance the fibre-optic materials and the piezoelectric-ceramic (PZT), have enabled online monitoring with greater resolution and quicker response as these materials have enormous competences of damage diagnosis. In recent times, sensors based on PZT and optical fibres have been studied for corrosion assessment in steel reinforced concrete structures [75–77].

Recently, an optical fibre sensor comprising of a fibre bragg grating sensor has been developed to identify steel rebar corrosion. A correlation between the weight loss rate of rebar (by gravimetric loss method) and reflected wavelength change from the grating was found through a series of accelerated corrosion tests. Through this relationship, it was noticed that the greater the wavelength shift, the larger the weight loss rate in the steel rebar [78]. Various analytical and experimental investigation have been carried out to detect rebar corrosion in steel reinforced concrete structures using fibre optic sensors [79–82]. Moreover, numerous proof-of-concept research to identify corrosion using PZT patches in metallic structures have been reported [77, 83]. However, these investigations were preliminary in nature and did not

offer any solid means of rigorous qualification of corrosion damage after its detection. Hence, more investigations are required in this field.

2.10 Comparison of different techniques

Since potential measurement, resistivity measurement and sensors techniques do not provide the corrosion rate of the steel reinforcement, therefore the comparison of corrosion rate as obtained from electrochemical and weight loss measurement techniques can be made based on past studies.

Ismail et al. [49] evaluated the corrosion condition of steel rebar in high performance concrete using potentiodynamic polarization (PP), electrochemical impedance spectroscopy (EIS), linear polarization resistance (LPR) techniques, and observed that the corrosion rates obtained from the LPR were 5–20% less than those obtained using EIS but 10–30% more than those determined using PP. Nygaard et al. [84] investigated the corrosion rate of passive steel and active steel by means of galvanostatic pulse (GP) and LPR techniques. They found that both GP and LPR methods overestimated the actual corrosion rate for passive steel by factors of about 100 and 10 times, respectively. But these methods underestimated the corrosion rates by a factor of 2 (GP) and 10 (LPR) for steel rebars with localized corrosion. Aligizaki [85] assessed the corrosion rate of steel using LPR, PP and EIS and found well correlation between the I_{corr} values obtained from LPR and PP techniques. Sathyanarayanan et al. [86] measured the corrosion rate of steel rebar by GP and LPR techniques and concluded that the GP technique provides more reliable corrosion rates than LPR method, when compared with the gravimetric weight loss method results. Law et al. [87] also used gravimetric weight loss and LPR methods to measure the corrosion rates of steel at regular intervals during an exposure period of 1,085 days. They compared the corrosion rates obtained from both the techniques and concluded that the LPR technique overestimated the corrosion rate. Pradhan et al. [88] observed that the corrosion rates obtained from LPR technique were 10% higher than those from the EIS method, whereas agreed closely with that found from the gravimetric weight loss method.

There are numerous existing techniques for the detection, measurement and diagnosis of corrosion of steel rebar, however there is no consent regarding which technique evaluates the corrosion rate more precisely. Therefore a combination of evaluating methods is recommended to use in order to find the reliable information about the corrosion condition of steel embedded in concrete. The average corrosion rate as obtained from the different techniques may be used for further analysis.

3 Corrosion control techniques

The corrosion control methods for steel reinforced cementitious composite include cathodic protection, electrochemical chloride extraction, surface treatments of the steel reinforcement, surface treatment of concrete, utilization of mineral admixtures and chemical corrosion inhibitors. In the subsequent sections, these methods have been discussed comprehensively.

3.1 Cathodic protection

The first investigation on corrosion control of steel in a reinforced concrete bridge through cathodic protection was reported by Stratfull in 1957 [89], and the application of this technique began in 1972 in order to protect Sky Park bridge decks contaminated by de-icing salts in Placerville, California [90]. Thereafter, research has been carried out by various government and private industries for the development of cathodic protection systems in steel reinforced concrete structures. For example, on the basis of research investigations, Federal Highway Administration has identified that the cathodic protection is the only rehabilitation system that has proven to stop corrosion in chloride contaminated bridge decks irrespective of the chloride content in concrete [91].

The cathodic protection system can be established by two ways: galvanic (sacrificial) anode and impressed current systems. The galvanic anode system is based on the principles of dissimilar metal corrosion and the relative position of specific metals in the electro-chemical series. Hence, this system employs reactive metals as auxiliary anodes, which are connected to the steel that is to be protected. The difference in potentials between the reactive metal and the steel, as specified by their relative positions in the electro-chemical series, causes a positive current to flow in the electrolyte, from the reactive metal to the steel. Thus, the whole surface of the steel converted to negatively charge and becomes the cathode. The metals commonly used, as sacrificial anodes are aluminium, zinc and magnesium. No external power source and low maintenance is required in this system. Patch-repair and plug-type anodes are examples of galvanic anodes [92].

In contrast, an impressed current system requires a current source (generally less than 50 volts) and inert (zero or low dissolution) anode material, fixed either on the surface, or embedded within the concrete. To achieve an electrical circuit, the positive terminal is connected to anode material and the negative terminal is connected to steel (cathode) to be protected, the anode and cathode are separated by an electrolyte (concrete) as shown in Fig. 12. This

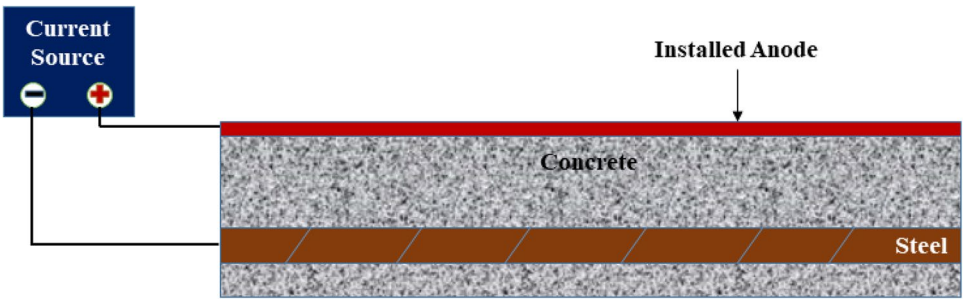

Fig. 12 Impressed current cathodic protection system [93]

system works well until power supply is not interrupted. Therefore, this system consumes substantial electrical energy and also requires specialized services to design and verify the system's functioning [93].

3.2 Electrochemical chloride extraction

The aim of the electrochemical chloride extraction (ECE) technique is to remove the chloride ions from the steel rebar and out of the concrete body. This method is similar to cathodic protection, but there are two main differences. First, the current density used for impressed current cathodic protection (ICCP) is much lower than that for ECE. Second, the external anode for ECE is temporary and installed for few weeks only (during the process) [94]. However, both protection techniques have been recognized to increase the service lifespan of the structures. However, ECE technique is more advantageous because of no long-term regular maintenance requirement.

In this technique, an electric field is applied between the steel reinforcement and an external anode metal fixed to the surface of the concrete body. The commonly used anodes are titanium-activated meshes, steel meshes, and mortar pastes prepared with graphite powder [95]. The positive terminal of current source is connected to anode, while negative terminal is connected to steel rebar embedded in concrete. When the electric current is applied, anions (such as Cl^-) are attracted towards the external anode placed on the surface of the concrete, while cations (such as Na^+, K^+) are migrated towards steel reinforcement and thereby produced hydroxyl ions (OH^-) on the surface steel, as a result of cathodic reactions. The schematic diagram of the chloride extraction technique is shown in Fig. 13. The following reactions occur during electrochemical extraction treatment due to the development of electric potential difference between the external anode and the steel (cathode) [96].

At anode:

$$2H_2O_{(l)} \rightarrow 4\,H^+_{(aq)} + O_{2(g)} + 4e^- \quad (14)$$

$$2Cl^-_{aq} \rightarrow Cl_{2(g)} + 2e^- \quad (15)$$

The pH of the electrolyte should be sufficiently high in order to suppress the reaction represented by Eq. (15). The highly alkaline electrolytes also neutralize the hydrogen ions produced by the reaction in Eq. (14) and protect the surface of concrete from acidification. Therefore, solution of calcium hydroxide, sodium hydroxide and treated water are commonly used as external electrolytes [97]. However, water is the most widely used owing to the deficiency of salts, thus Cl^- ions travel more easily in the concrete and are extracted effortlessly [98].

At cathod (steel):

$$O_{2(g)} + 2H_2O_{(l)} + 4e^- \rightarrow 4OH^-_{(aq)} \quad (16)$$

$$H_2O_{(l)} + 2e^- \rightarrow 2OH^-_{(aq)} + H_{2(g)} \quad (17)$$

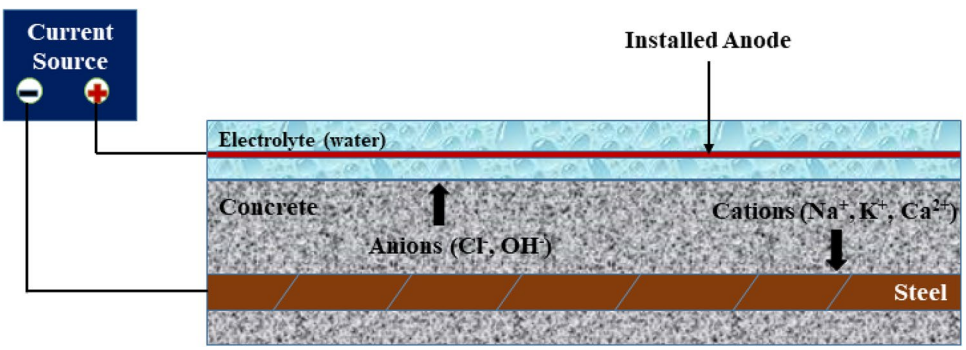

Fig. 13 Illustration of the chloride extraction technique [96]

The Eq. (17) shows the evolution of hydrogen gas at the level of steel reinforcement due to the low cathodic potential that is induced by the high current density. Also, it is believed that higher current densities can produce cracking in the concrete as a function of the chloride extraction velocity. Therefore, the current density has been taken between 1 A/m^2 and 5 A/m^2 in various studies [94]. Despite this, some authors determine that the current density should not be more than 2 A/m^2 [99]. However, some of the studies focused on densities up to 1 A/m^2 [100].

The period of application of this system varies from 6 to 10 weeks [101], in this period the chloride concentration is reduced below 0.4% of total chlorides, which is considered as critical value [102]. According to results of an investigation, the chloride content was found to be reduced by around 40% within 7 weeks of treatment and simultaneously, substantial quantities of alkali ions were detected nearby the steel [103]. The reduction percentage of chloride content can reach up to 70% [104]. The reduction of chloride ions content below the critical level and simultaneous increment of hydroxyl concentration on the surface of the steel reinforcement creates favourable environment for the steel repassivation [105].

3.3 Surface treatment of steel

The reinforcing bars commonly used are mild steel, mainly due to its significant low cost. Alternatively, stainless steel shows excellent mechanical and durability properties, but impractical for use in reinforced concrete because of its high cost [106]. The poor corrosion resistance of mild steel is a common cause of deterioration in reinforced concrete structure. Therefore, various treatments have been given to steel surface in order to increase the corrosion resistance. One such treatment is coating with epoxy, which acts as a barrier to aggressive corrosion agents, and thus significantly decrease the corrosion rate of steel rebar. But, the poor bonding between epoxy coated steel and concrete, and the damaged areas of epoxy coated steel rebar (at which pitting corrosion may occur) are the common problems with epoxy coating [107]. Another similar treatment is coating with zinc (*galvanization*), which improve the corrosion resistance of steel by acting as a sacrificial anode. It has been observed in many studies that the galvanized steel develops better bond to concrete than the epoxy coated steel, and also the tendency of the zinc coating to debond is very less as compared to epoxy coating [108]. Subsequently, techniques for surface treatment of steel that increases the corrosion resistance as well as bond strength have been developed. These techniques include inhibited cement slurry coating, surface oxidation and sand blasting.

The Central Electrochemical Research Institute (CECRI), Karaikudi, India, has developed inhibited cement slurry coating for corrosion control in steel reinforcement. This coating system involves of four stages i.e. pickling, phosphating, two times application of inhibited cement slurry coating and sealing. This coating is an in situ process that is carried out after all bending and shaping operations are completed at the construction site. As this coating is applied at the site of working, the damage caused on account of transporting and lifting are significantly minimised. Moreover, in situ patch repairing is easy to execute in this coating system. Though, strict quality control measures are required to ensure the performance of this coating [109]. In an investigation, it was concluded that the inhibited cement slurry coating is economical and efficient to control the corrosion of steel reinforcement [110]. In an another study, it was observed that inhibited cement slurry coated steel show higher bond strength as compared to galvanized and epoxy coated steel [111].

Sand blasting technique involves the blasting of Al_2O_3 particles (size about 250 μm) on the steel rebar under pressure of around 0.6 MPa. It is used for cleaning of the surface of the steel. The cleaning includes the removal of rust and/or contaminants from the surface of steel. This cleaning improves the corrosion resistance by making the surface of the steel more uniform in composition. Moreover, the cleaning increases the roughness of surface and thus improves the bond strength. However, the disadvantage of this method is that it is uneconomical and difficult to use in the construction site [112].

Water immersion method involves the immersion of the steel rebar under water at ambient temperature for 2 days. This treatment forms a black coating (oxide layer) on the steel surface, hence the surface of steel turns out to be more uniform in composition and thereby, enhancing the corrosion resistance. Furthermore, the oxide layer improves the bond between concrete and rebar, thus increasing the bond strength. The immersion periods less than or more than 2 days provide less beneficial effects on both corrosion resistance and bond strength. This method is found to be very simple and economical as compared to other methods [113].

3.4 Surface treatment of concrete

Since numerous hostile agents (e.g. chloride, CO_2 etc.) ingress into the concrete through air or water and creates durability problems (e.g. carbonation, chloride attack and sulphate attack etc.), therefore, the permeation property of the surface concrete is considered as a main factor that impact the durability of entire concrete structure [114].

Concrete surface treatment has gained sufficient attention since 1980s, for example, American and German transportation agencies applied some hydrophobic agents on the surface concrete of bridges in order to prevent

chloride penetration. Also, a chemical named isobutiltrimetoxisilane (100% pure and hydrophobic agent) has been used on bridges in the United Kingdom in 1986 to protect from chloride attack [115]. However, many progresses has been occurred in terms of understanding the mechanism of already known surface treatment agents; and various new treatment agents has emerged in last two decades. Moreover, the surface treatment agents can be classified into two categories based on chemical composition i.e. organic and inorganic. Organic agents are widely used for surface treatment of concrete owing to their good barrier properties. But, there are some problems associated with organic treatments viz. poor fire resistance, crack and detach easily, inadequate service life, and after losing protecting effects their removal is difficult [116].In contrast, the inorganic surface treatment agents are more stable and have better durability performance. The most commonly used inorganic surface treatment agent is sodium silicate. Also, it has been reported that lithium silicate, potassium silicate and fluosilicates can be used as inorganic surface treatment agents for concrete [117].

According to the functions of surface treatments, they were grouped into four types: surface coating, hydrophobic impregnation, pore blocking treatment and multifunctional surface treatments [118]. Surface coating forms a continuous layer and produce a physical barrier to prevent the ingress of the corrosive substances into cementitious substrate [119]. There are many types of surface coatings which have been used in the construction industry, for example, acrylic, chlorinated rubber, butadiene copolymer, polyethylene copolymer, epoxy resin, polyester resin, vinyl, polyurethane, coal tar and polymer modified cementitious coatings [120].

Hydrophobic impregnation works via penetrating concrete pores, expanding the contact angle. The surface turns out to be hydrophobic when the contact angle is greater than 90°. Thus, hydrophobic impregnation can prevent the ingress of water and water-born ions; but permits penetration of water vapour [113]. The most commonly used hydrophobic impregnation are silane, siloxane and a combination of these two chemicals. The molecular structures of silane (1.0 to 1.5 μm diameter) and siloxane (1.5 to 7.5 μm diameter) are extremely small; and therefore, efficiently penetrate into dense concrete substrate. Both silane and siloxane comprise an alkyl group and various alkoxy groups [121, 122]. The alkyl group can decrease the surface tension of the substrate, whereas the alkoxy group is related to the bonds between silane/siloxane and concrete. For example, the chemical reaction between silane and concrete substrate can be proceeded as: firstly, silane hydrolysis reacts with pore water, and silanol groups are formed due to hydrolysis alkoxy groups [123]. Then, the unstable silanol molecules lose water molecules and transformed into silicone resin. Subsequently, the silanol groups react with hydroxyl groups in the cementitious substrate via hydrogen bonds. Lastly, the silicon resin bonds to cementitious substrate during drying, and creates water repellent pore surfaces. The alkalinity of the cementitious substrate serves as a catalyst in these reactions [124].

Pore blocking surface treatment agents have been used in construction industries for many years [125]. They are able to partially or completely block the existing capillary pores in concrete surface and thus increase impermeability of surface layer. Silicate and fluosilicate based pore blockers (e.g. calcium silicate, lithium silicate, sodium silicate, magnesium fluosilicate and sodium fluosilicate) have been demonstrated to be effective in blocking capillary pores in concrete surfaces. Sodium silicate is considered as one of the most common pore blocking agents [126].

Multifunctional surface treatments should have at least two functions, for example, ethyl silicate (or tetraethylorthosilicate), an alkoxysilane compound, which itself does not have binding property, and nevertheless it can produce silica gels and block the pores through hydrolysing process. Also, it can prevent the entry of corrosive substances because of its hydrophobic effect [127]. Similarly, Silane-clay nanocomposites are not only show a hydrophobic effect, but also improve the microstructure of concrete cover [128].

Surface treatment of concrete may be an effective and economical technique in order to enhance the quality of surface concrete and improve the durability of concrete structures. However, this technique of corrosion control suffers from the poor durability of the coating and the loss of corrosion protection in the parts where the coating is damaged.

3.5 Admixtures in concrete

Admixtures are solid or liquid substances that are added to the concrete mixture in order to enhance the properties of the resulting concrete. Admixtures that are primarily used for improving the corrosion resistance of steel reinforcement, commonly known as corrosion inhibitors. These include mainly organic and inorganic chemicals. However, admixtures that are mainly used for enhancing the structural performance of concrete are more attractive due to their multi-functionality (such as, improvement in workability, mechanical strengths, bond strength, impermeability, corrosion control, etc.). They are usually mineral particles, for example, fly ash, silica fume and slag.

Fly ash (FA) is a by-product of coal combustion and mainly composed of SiO_2 and CaO. The recent advancement in concrete technology exhibits that the fly ash is the most common pozzolan and used worldwide as an essential component for making high-performance concrete. This is mainly because of pozzolanic reaction between fly ash and hydrated cement paste resulting a denser microstructure over a period of time. However, studies

have revealed that fly ash does not reduce the diffusion coefficient of concrete at early ages, but at the later ages, significantly lowers the diffusion coefficient as compared to control concrete [129]. Moreover, Class F fly ash (low CaO content) leads to a slightly lower diffusion coefficient than Class C fly ash (high CaO content) admixed concrete [130]. As far as steel reinforcement corrosion is concerned, it was observed that the corrosion resistance of steel in concrete is improved with the addition of fly ash as a replacement of Portland cement (PC) up to the 30% [131]. In another study, it was concluded that the incorporation of 15% fly ash as replacement of cement can produced quite durable concretes against corrosion [132]. Also, it was found that the chloride penetration resistance of concrete increases with increasing the fineness of fly ash [133]. In general, it is recognised that the addition of fly ash improves the corrosion resistance properties of steel reinforcement by reducing porosity and increasing the resistivity of cementitious composite [134]. Moreover, fly ash is typically used at replacement levels between 15% and 35% by weight of Portland cement so as to increase the mechanical strengths as well as the resistance to deterioration mechanisms (such as chloride attack, sulphate attack, carbonation etc.) of cementitious composites [135].

Silica fume (SF) is a by-product from silicon alloy production in electric arc furnaces. It is almost pure SiO_2 and its particles size are approximately 100 times finer than cement grains. When added in cementitious composite, silica fume reacts quickly with hydrated cement due to small particle size and high surface area to volume ratio and consequently improving the microstructural and mechanical properties and decreasing the diffusion coefficient of cementitious composite at all ages with respect to plain cementitious composite [110, 111]. Though, it was observed that chloride diffusion coefficient of concrete in a marine environment reduces with lowering the water binder ratio and increasing silica fume content up to 10%. Also, the chloride diffusion coefficient is found to be high for early ages and drops over time [138]. The reduction in diffusivity leads to decrease the chloride threshold level required to initiate corrosion, and this may increase the service life of the exposed concrete structures by 15-fold in certain circumstances [139]. From the sensitivity analysis, it is calculated that with the addition of 10% silica fume in concrete, the chloride transport in terms of apparent diffusion coefficient is reduced by approximately 74% and corrosion-free life is increased by 270% as compared to OPC concrete [140]. Moreover, the incorporation of silica fume in appropriate quantity, significantly enhances the corrosion resistance properties of steel reinforced cementitious composite [115, 116]. Furthermore, the typical replacement levels of Portland cement with silica fume range from 3% to 10% in order to enhance the mechanical strengths and durability properties of concrete structures [134].

Ground granulated blast-furnace slag (GGBFS), commonly known as slag, is a by-product of steel production. It mainly contains CaO, SiO_2, Al_2O_3 and MgO [143]. When slag is used as part of Portland cement in concrete, it reacts with both the hydrated cement (*pozzolanic reaction*) and the water (*latent hydraulic reaction*), and consequently refined the pore structure and enhanced interfacial transition zone (ITZ) of concrete [144]. Also, the addition of slag, improves the consistency and workability of fresh concrete. The mechanical strengths and durability properties of concrete is found to be substantially improved with the incorporation of GGBFS [145]. The diffusion coefficient of GGBFS admixed cementitious composite is found to be significantly lower as compared to the plain cementitious composite, particularly at the later exposure ages. Therefore, when incorporated appropriate amount of GGBFS in concrete, the transportation of corrosive agents is greatly reduced and consequently improved the corrosion resistance of steel reinforcement, and thereby, increasing the predicted service life of concrete structures. From most of the investigational studies, it may be concluded that the use of 40% to 80% of GGBS as a replacement of Portland cement does not cause any negative impact on the performance of cementitious composite [120, 121].

Metakaolin (MK) is obtained by the calcination of clay mineral kaolinite ($Al_2Si_2O_7$) at the temperature range of 500 °C to 800 °C. It is primarily composed of SiO_2 and Al_2O_3. The size of 99.9% metakaolin particles is below 16 μm and the average particle size is approximately 3 μm. It is a pozzolanic material and commonly used in the manufacture of ceramics [148]. The small particle size, high surface area to volume ratio and pozzolanic property of metakaolin, make it possible to be befittingly used as partial replacement of cement up to 10% and fine aggregate up to 20% in concrete [149]. The studies revealed that when metakaolin is used in concrete, it reacts quickly due to small particle size and high surface area, and undergoes pozzolanic reaction, and consequently improves the microstructure of the hydrated cement paste [150]. This improvement leads to further enhancement in the mechanical and durability properties and reduction in the diffusion coefficient of concrete [151]. In particular, the corrosion resistance of steel reinforcement in aggressive environment is improved substantially with the inclusion of suitable amount of metakaolin. Besides, the appropriate replacement level of cement by metakaolin ranges from 5 to 10% [152].

Moreover, the use of binary blends (Portland cement plus one admixture, such as PC + SF, PC + SF, PC + GGBFS and so on.) and ternary blends (Portland cement plus two admixtures, such as PC + FA + SF, PC + MK + FA, PC + FA + GGBFS etc.) can significantly enhance the performance of cementitious composite exposed to corrosive environments. Research has revealed that the use of

admixtures can reduce the diffusion coefficient of concrete and consequently improve the corrosion resistance of steel reinforcement. However, it has been observed that ternary blends result in superior resistance to chloride ingress compared with binary blends at both early and later ages. This is because the ternary blends contain a slow-reacting admixture (e.g. fly ash or slag) and a fast-reacting admixture (e.g. silica fume or metakaolin) [153]. In addition, such replacement of cement will contribute to the reduction in CO_2 production (carbon footprint) and therefore encourage the use of such sustainable and green concrete. Furthermore, recently some new generation nano-admixtures (such as carbon nanotubes, SiO_2, TiO_2, Fe_2O_3, CuO, ZrO_2, ZnO_2, Al_2O_3, $CaCO_3$, Cr_2O_3) emerges, which can be used to improve the microstructure and corrosion resistance properties of reinforced concrete [154].

3.6 Chemical corrosion inhibitors

International Organization for Standardization (ISO 8044:2015) defines corrosion inhibitor as a chemical substance that decreases the corrosion rate when present in the corrosion system at suitable concentration, without significantly changing the concentration of any other corrosion agent [155]. The National Association of Corrosion Engineers (NACE) defines corrosion inhibitors as substances that, when added to an environment, decrease or slow down the rate of attack of the metal [156]. ACI 116R-85 defines a corrosion inhibitor as a chemical compound, either liquid or powder, that effectively decreases or slows down reinforcement corrosion in hardened concrete if introduced, usually in very small concentrations, as an admixture [157]. Therefore, an ideal corrosion inhibitor for cementitious composite may be defined as a chemical compound, which, when incorporated in suitable quantities to cementitious composite, can control corrosion of embedded steel reinforcement and has no adverse effect on the fresh and hardened properties of cementitious composite [158]. These definitions exclude other corrosion control methods such as pore blockers, coatings etc., which modify the oxygen, water and chloride concentrations. Nevertheless, some chemical corrosion inhibitors may also act as pore blockers, which is a secondary property. The inhibitors may be the better than the other methods of protection owing to lower cost and easy to use.

The inhibitors could be classify in many ways: according to their application methods, according to their mechanism of protection, and their chemical nature [132, 133]. The main application methods for corrosion inhibitors are:

(a) Added to fresh concrete as an admixture
(b) Added to repair mortars
(c) Used as a surface treatment on the steel reinforcement bars before concreting
(d) Applied on the hardened concrete surface, as a penetrating corrosion inhibitor (also surface-applied corrosion inhibitor and migrating corrosion inhibitor).

According to the mechanisms of protection, corrosion inhibitors could be divide into three types:

(a) Anodic inhibitors: These inhibitors passivate the metal by forming a film adsorbed or insoluble layer on anodic surfaces of the metal. They mainly act by affecting the anodic reaction and consequently reducing the corrosion rate by increasing the corrosion potential and decreasing the corrosion current density of the metal. Though, the sufficient concentration of anodic inhibitors must be used for covering the entire surface of metal. The inappropriate concentration of inhibitors affects the formation of film and leaves some exposed sites, and thus causes pitting corrosion. The commonly used anodic inhibitor are nitrites, nitrates, benzoates, chromates, molybdates, phosphates, hydroxides, silicates and carbonates.
(b) Cathodic inhibitors: These inhibitors act by forming a barrier of insoluble precipitates over the metal surface and particularly affecting the cathodic reaction. Accordingly, reduced the corrosion rate by decreasing the corrosion potential as well as corrosion current density of metal. These inhibitors are usually less effective but more secure than anodic inhibitors. Examples of cathodic inhibitors are silicates, phosphates polyphosphates, tannins and ions of the zinc, nickel and magnesium that react with the hydroxyl (OH^-) of the water forming the insoluble hydroxides as $Zn(OH)_2$, $Ni(OH)_2$, $Mg(OH)_2$, which are deposited on the cathodic site of the metal surface, protecting it.
(c) Mixed inhibitors: These inhibitors act on both anodic and cathodic sites by adsorption on overall surface of the metal. They reduce the corrosion rate by decreasing the corrosion current density without substantial changing the corrosion potential of metal. This type of inhibitor includes amines, amino alcohols, sulfonates, esters and compound with the hydrophobic group that have polar groups such as N, S and OH.

According to chemical functionality, the inhibitors can be classified as follows:

(a) Inorganic Inhibitors: These inhibitors are generally crystalline salts such as nitrite salts, chromate salts, molybdate compounds, zinc salts, phosphates, silicate compounds etc. Usually, the anions of these salts are involved in decreasing the corrosion of metal. In general, these inhibitors have anodic or cathodic actions. However, when zinc salt is used, the zinc cation can

add some advantageous effect. These zinc-added salts are termed as mixed-charge inhibitors.

(b) Organic Inhibitors: The inhibitors are characterized by high molecular weight structures, incorporating $–NH_2$, –SH, –COOH, –OH or $–SO_3H$ functional groups. In their concentrated forms, these are either liquids or wax like solids. Their active portions are generally large aliphatic or aromatic compounds with positively charged amine groups. These inhibitors are said to be chelating agents, which can form five or six-membered chelate rings. These rings are formed as a result of the bonding between two or more functional groups from the inhibitor and the cation metal, thus, completely cover the metal surface. However, occasionally, they act as cathodic, anodic or mixed inhibitors. Some examples are amines, mercaptobenzothiazole, aldehydes, sulphur-containing compounds, heterocyclic nitrogen compounds and acetylenic compounds.

As compared to the other corrosion control techniques, chemical corrosion inhibitors have some benefits such as economical and versatility. Application of inhibitors in concrete can aid to delay the corrosion initiation in the embedded steel exposed to aggressive environments. However, after the corrosion initiation, their efficiency was less significant. In general, the side effects of the inhibitors on fresh and hardened concrete were reported to be insignificant [161]. Very limited studies on the long-term performance of the inhibitors in real structures are available. Hence, more researches are needed to identify such inhibitors that are effective throughout the service life of structures and are non-hazardous.

4 Conclusions

From the critical review discussed concerning steel rebar corrosion monitoring and controlling techniques, following points can be noted

(1) Potential measurements have been extensively used since 1970 to assess the corrosion risk of steel rebar in concrete. Though, potential values do not provide the corrosion rate of steel. In spite of the simple method for potential measurement on the surface of concrete, the potential mapping results need cautious interpretation. Also, the depth of concrete cover, concrete resistance, polarization effects and high resistivity of surface layer significantly influence the measured potential values.

(2) The corrosion rate can be evaluated using electrochemical techniques such as potentiodynamic polarization, linear polarization resistance, galvanostatic pulse, electrochemical impedance spectroscopy, Tafel extrapolation. These techniques can be used in small steel reinforced concrete specimens under laboratory environments as well as large scale field structures. However each method possesses certain advantages and limitations. Therefore a combination of evaluating methods is recommended to use in order to find maximum information about the corrosion condition of steel embedded in concrete.

(3) The gravimetric weight loss measurements is an efficient technique for finding the corrosion rate of steel rebars, but it is destructive and is usually performed after long exposure times

(4) Potential measurement, electrical resistivity measurement and sensors techniques do not provide the corrosion rate of the steel reinforcement, they only give qualitative information. However, corrosion monitoring using PZT and optical-fibre sensors is still a new area of research and needs to be explored. Although some of the researchers considered that there is a robust potential in emerging the sensors as a non-destructive method for corrosion assessment that can be possibly provide better assessment than the conventional methods.

(5) The corrosion control methods for steel reinforced concrete include cathodic protection, electrochemical chloride extraction, surface treatments of the steel reinforcement, surface treatment of concrete, utilization of mineral admixtures and chemical corrosion inhibitors. Each method possesses certain advantages and disadvantages. Consequently, more researches are needed to develop such methods of corrosion protection of embedded steel that are economical, durable, environment-friendly and do not cause any adverse effect on the structural performance of concrete and steel.

Acknowledgments Md Daniyal is thankful to the Council of Scientific and Industrial Research (CSIR), Human Resource Development Group, Government of India, for providing financial assistance in the form of JRF and SRF.

Compliance with ethical standards

Conflict of interest The authors declare that they have no conflict of interest.

References

1. Lazell EW (1915) Hydrated lime: history, manufacture and uses in plaster, mortar, concrete; a manual for the architect, engineer, contractor and builder. Jackson-Remlinger Print. Co., Pittsburgh
2. Searle AB (1935) Limestone and its products: their nature, production, and uses. Ernest Benn Ltd., London

3. Gagg CR (2014) Cement and concrete as an engineering material: an historic appraisal and case study analysis. Eng Fail Anal 40:114–140
4. Singh DDN, Venugopalan T (2013) Understanding the corrosion and remedial measures to control the deterioration of reinforcement steel bars by modification in their chemistry and application of surface coatings. Trans Indian Inst Met 66:677–687
5. Zhao Y, Jin W (2016) Chapter-1 steel corrosion-induced concrete cracking (China Science Publishing & Media Ltd. Published by Elsevier) pp 1–17
6. Anon (2000) The effects and economic impact of corrosion. Corrosion: Understanding the Basics (ASM International) pp 1–20
7. Koch GH, Brongers MPH, Thompson NG, Virmani YP, Payer JH (2002) Corrosion costs and preventive strategies in the United States NACE Int. FHWA-RD-01 1–12
8. Koch G, Varney J, Thompson N, Moghissi O, Gould M, Payer J (2016) International measures of prevention, application, and economics of corrosion technologies study. NACE Int. 1–216
9. Song H, Saraswathy V (2007) Corrosion monitoring of reinforced concrete structures—a review. Int J Electrochem Sci 2:1–28
10. ASTM C876—15 2015 standard test method for corrosion potentials of uncoated reinforcing steel in concrete
11. Perveen K, Bridges GE, Bhadra S, Thomson DJ (2014) Corrosion potential sensor for remote monitoring of civil structure based on printed circuit board sensor. IEEE Trans Instrum Meas 63:2422–2431
12. Erdoğdu Ş, Kondratova IL, Bremner TW (2004) Determination of chloride diffusion coefficient of concrete using open-circuit potential measurements. Cem Concr Res 34:603–609
13. Razak HA, Choi FC (2001) Damage assessment of corroded reinforced concrete beams using modal testing. Structural Engineering, Mechanics and Computation (Elsevier) pp 1203–15
14. Choi YS, Kim JG, Lee KM (2006) Corrosion behavior of steel bar embedded in fly ash concrete. Corros Sci 48:1733–1745
15. Yeih W, Huang R (1998) Detection of the corrosion damage in reinforced concrete members by ultrasonic testing. Cem Concr Res 28:1071–1083
16. Elsener B, Andrade C, Gulikers J, Polder R, Raupach M (2003) Half-cell potential measurements—Potential mapping on reinforced concrete structures. Mater Struct 36:461–471
17. Gu GP, Carter P, Beaudoin JJ, Arnott M (1996) Validation of half-cell potential data from bridge decks. Constr Repair 10:18–20
18. Elsener B (2001) Half-cell potential mapping to assess repair work on RC structures. Constr Build Mater 15:133–139
19. Butler JAV (1924) Studies in heterogeneous equilibria. Part III. A kinetic theory of reversible oxidation potentials at inert electrodes. Trans Faraday Soc 19:734–739
20. Erdey-Gruz T, Volmer M (1930) The theory of hydrogen overvoltage *Z.* Phys Chem 150:203–213
21. Frankel GS (2016) Active protective coatings vol 233. In: Hughes AE, Mol JMC, Zheludkevich ML, Buchheit RG (ed) Springer Netherlands, Dordrecht
22. Tafel J (1905) Über die Polarisation bei kathodischer Wasserstoffentwicklung. Z Phys Chem 50:641–712
23. Zhang XL, Jiang ZH, Yao ZP, Song Y, Wu ZD (2009) Effects of scan rate on the potentiodynamic polarization curve obtained to determine the Tafel slopes and corrosion current density. Corros Sci 51:581–587
24. Anon 2004 ASTM G 5—94, Standard reference test method for making potentiostatic and potentiodynamic anodic polarization measurements
25. Munir S, Pelletier MH, Walsh WR (2016) Potentiodynamic corrosion testing J Vis Exp
26. Jarrah NR, Al-amoudi OSB, Ashiru OA, Al-mana A (1995) Electrochemical behaviour of steel in plain and blended cement concretes in sulphate and/or chloride environments. Constr Build Mater 9:97–103
27. Yu H, Chiang KK, Yang L (2012) Threshold chloride level and characteristics of reinforcement corrosion initiation in simulated concrete pore solutions. Constr Build Mater 26:723–729
28. Aldabbagh BM, Alshimary HJ (2017) Polyamide nanofibers coating by electrospinning technique for anti corrosion behavior. Eng Technol J 35:987–991
29. Saremi M, Mahallati E (2002) A study on chloride-induced depassivation of mild steel in simulated concrete pore solution. Cem, Concr Res 32:1915–1921
30. Ghods P, Isgor OB, Mcrae GA, Gu GP (2010) Electrochemical investigation of chloride-induced depassivation of black steel rebar under simulated service conditions. Corros Sci 52:1649–1659
31. Mahallati E, Saremi M (2006) An assessment on the mill scale effects on the electrochemical characteristics of steel bars in concrete under DC-polarization. Cem Concr Res 36:1324–1329
32. Stern M, Geary AL (1957) Electrochemical polarization-I. A theoretical analysis of the shape of polarization curves. J Electrochem Soc 104:56–63
33. Stern M (1957) Electrochemical polarization-II. Ferrous-Ferric electrode kinetics on stainless steel. J Electrochem Soc 104:559–563
34. Stern M (1957) Electrochemical polarization-III. Further aspects of the shape of polarization curves. J Electrochem Soc 104:645–650
35. Millard SG, Law D, Bungey JH, Cairns J (2001) Environmental influences on linear polarisation corrosion rate measurement in reinforced concrete. NDT E Int 34:409–417
36. Anon 2016 Linear polarization resistance and corrosion rate-Theory and background Pine Res. Instrum. DRA10086 1–14
37. Castillo FB, Roa-rodríguez G, Cabrera CC, Melo N, Aperador W (2015) Determination of the probability and rate of corrosion on reinforced concrete specimens through a remote corrosion monitoring system. Tecciencia 10:27–31
38. Anon 2009 ASTM G59-97: Standard test method for conducting potentiodynamic polarization resistance measurements
39. Natarajan P, Ramakrishnan KR (2007) LPR meter for concrete corrosion studies. J Instrum Soc India 37:1–6
40. Andrade C, Alonso C, Polder R, Cigna R, Vennesland Ø, Salta M, Raharinaivo A, Elsener B (2005) Test methods for on-site corrosion rate measurement of steel reinforcement in concrete by means of the polarization resistance method. Mater Struct 37:623–643
41. Dehwah HAF, Maslehuddin M, Austin SA (2002) Long-term effect of sulfate ions and associated cation type on chloride-induced reinforcement corrosion in Portland cement concretes. Cem Concr Compos 24:17–25
42. Goni S, Andrade C (1990) Synthetic concrete pore solution chemistry and rebar corrosion rate in the presence of chlorides. Cem Concr Compos 20:525–539
43. Glass GK, Buenfeld NR (1997) Presentation of the chloride threshold for corrosion of steel in concrete. Corros Sci 39:1001–1013
44. Huang QA, Hui R, Wang B, Zhang J (2007) A review of AC impedance modeling and validation in SOFC diagnosis. Electrochim Acta 52:8144–8164
45. Ribeiro DV, Souza CAC, Abrantes JCC (2015) Use of Electrochemical Impedance Spectroscopy (EIS) to monitoring the corrosion of reinforced concrete. Rev Ibracon estruturas e Mater. 8:529–546
46. Anon ASTM-STP1065-Study of the corrosion of concrete reinforcement by electrochemical impedance measurement

47. Ribeiro DV, Abrantes JCC (2016) Application of electrochemical impedance spectroscopy (EIS) to monitor the corrosion of reinforced concrete: a new approach. Constr Build Mater 111:98–104
48. Martínez I, Andrade C (2008) Application of EIS to cathodically protected steel: tests in sodium chloride solution and in chloride contaminated concrete. Corros Sci 50:2948–2958
49. Ismail M, Ohtsu M (2006) Corrosion rate of ordinary and high-performance concrete subjected to chloride attack by AC impedance spectroscopy. Constr Build Mater 20:458–469
50. Gu GP, Beaudoin JJ, Ramachandran VS (2001) Techniques for corrosion investigation in reinforced concrete-Handbook of analytical techniques in corrosion science and technology. Noyes Publications, New Jersey
51. Newton CJ, Sykes J (1988) A galvanostatic pulse technique for investigation of steel corrosion in concrete. Corros Sci 28:1051–1074
52. Elsener B, Klinghoffer O, Frolund T, Rislund E, Schiegg Y, Böhni H (1997) Assessment of reinforcement corrosion by means of galvanostatic pulse technique Int. Conf. Repair of Concrete Structures", Svolvær, Norway pp 1–10
53. Klinghoffer O (1995) In situ monitoring of reinforcement corrosion by means of electrochemical methods. Nord Concr Res 95:1–13
54. Law DW, Millard SG, Bungey JH (1999) The use of galvanostatic pulse measurements to determine corrosion parameters. Durab Build Mater Comp. 8:310–319
55. Elsener B (2005) Corrosion rate of steel in concrete-measurements beyond the Tafel law. Corros Sci 47:3019–3033
56. Cavalier PG, Vassie PR (1981) Investigation and repair of reinforcement corrosion in a bridge deck. PI Civ Eng Part-1 70:461–480
57. Hope B, Ip AK, Manning DG (1985) Corrosion and electrical impedance in concrete. Cem Concr Res 15:525–534
58. López W, González JA (1993) Influence of the degree of pore saturation on the resistivity of concrete and the corrosion rate of steel reinforcement. Cem Concr Res 23:368–376
59. Hughes BP, Soleit AKO, Brierly RW (1985) New technique for determining the electrical resistivity of concrete. Mag Cem Concr Res 37:243–248
60. Hansson ILH, Hansson CM (1983) Electrical resistivity measurements of Portland cement based materials. Cem Concr Res 13:675–683
61. Buenfeld NR, Newman JB, Page CL (1986) The resistivity of mortars immersed in sea-water. Cem Concr Res 16:511–524
62. Wenner F 1916 A method of measuring earth resistivity *Bull. Bur. Stand.* 469–78
63. Chen CT, Chang JJ, Yeih WC (2014) The effects of specimen parameters on the resistivity of concrete. Constr Build Mater 71:35–43
64. Gowers KR, Millard SG (1999) Measurement of concrete resistivity for assessment of corrosion severity of steel using Wenner technique. ACI Mater J 96:536–541
65. Azarsa P, Gupta R (2017) Electrical resistivity of concrete for durability evaluation: a review. Adv Mater Sci Eng
66. Morris W, Vico A, Vazquez M, DeSanchez SR (2002) Corrosion of reinforcing steel evaluated by means of concrete resistivity measurements. Corros Sci 44:81–99
67. González JA, Miranda JM, Feliu S (2004) Considerations on reproducibility of potential and corrosion rate measurements in reinforced concrete. Corros Sci 46:2467–2485
68. Andrade C, Alonso C (1996) Corrosion rate monitoring in the laboratory and on-site. Constr Build Mater 10:315–328
69. Broomfield J, Millard S (2002) Measuring concrete resistivity to assess corrosion rates. Concrete 128:37–39
70. Smith K, Schokker A, Tikalsky P (2004) Performance of supplementary cementitious materials in concrete resistivity and corrosion monitoring evaluations. ACI Mater J 101:385–389
71. Pech-Canul MA, Castro P (2002) Corrosion measurements of steel reinforcement in concrete exposed to a tropical marine atmosphere. Cem Concr Res 32:491–498
72. Bertolini L, Carsana M, Pedeferri P (2007) Corrosion behaviour of steel in concrete in the presence of stray current. Corros Sci 49:1056–1068
73. Anon (2017) ASTM G1-03—Standard practice for preparing, cleaning, and evaluating corrosion test specimens
74. Chinwko EC, Odio BO, Chukwuneke JL, Sinebe JE (2014) Investigation of the effect of corrosion on mild steel in five different environments. Int J Sci Technol Res 3:306–310
75. Park S, Yun CB, Roh Y, Lee JJ (2006) PZT-based active damage detection techniques for steel bridge components. Smart Mater Struct 15:957–966
76. Park S, Grisso BL, Inman DJ, Yun CB (2007) MFC-based structural health monitoring using a miniaturized impedance measuring chip for corrosion detection. Res Nondestruct Eval 18:139–150
77. Park S, Park SK (2010) Quantitative corrosion monitoring using wireless electromechanical impedance measurements. Res Nondestruct Eval 21:184–192
78. Gao J, Wu J, Li J, Zhao X (2011) Monitoring of corrosion in reinforced concrete structure using Bragg grating sensing. NDT E Int 44:202–205
79. Fuhr PL, Huston DR (1998) Corrosion detection in reinforced concrete roadways and bridges via embedded fiber optic sensors. Smart Mater Struct 7:217–228
80. Grattan SKT, Basheer PAM, Taylor SE, Zhao W, Sun T, Grattan KTV (2007) Fibre Bragg grating sensors for reinforcement corrosion monitoring in civil engineering structures. J Phys Conf Ser 76
81. Grattan SKT, Taylor SE, Basheer PAM, Sun T, Grattan KTV (2009) Monitoring of corrosion in structural reinforcing bars: performance comparison using in situ fiber-optic and electric wire strain gauge systems. IEEE Sens J 9:1494–1502
82. Zheng Z, Sun X, Lei Y (2009) Monitoring corrosion of reinforcement in concrete structures via fiber Bragg grating sensors. Front Mech Eng China 4:316–319
83. Rathod VT, Roy Mahapatra D (2011) Ultrasonic Lamb wave based monitoring of corrosion type of damage in plate using a circular array of piezoelectric transducers. NDT E Int 44:628–636
84. Nygaard PV, Geiker MR, Elsener B (2009) Corrosion rate of steel in concrete: evaluation of confinement techniques for on-site corrosion rate measurements. Mater Struct Constr 42:1059–1076
85. Aligizaki KK (2007) Assessing corrosion rates of steel in chloride-contaminated concrete using different techniques. CORROSION NACE-07280 1–14
86. Sathiyanarayanan S, Natarajan P, Saravanan K, Srinivasan S, Venkatachari G (2006) Corrosion monitoring of steel in concrete by galvanostatic pulse technique. Cem Concr Compos 28:630–637
87. Law DW, Cairns J, Millard SG, Bungey JH (2004) Measurement of loss of steel from reinforcing bars in concrete using linear polarisation resistance measurements. NDT E Int 37:381–388
88. Pradhan B, Bhattacharjee B (2009) Performance evaluation of rebar in chloride contaminated concrete by corrosion rate. Constr Build Mater 23:2346–2356
89. Stratfull RF (1957) The corrosion of steel in a reinforced concrete bridge. Corrosion 13:43–48
90. Stratfull RF (1973) Preliminary investigation of cathodic protection of a bridge deck Calif. Dep. Transp. Sacramento, Calif

91. Barnhart RA (1982) FHWA position on cathodic protection (Washington, DC)
92. Bennett JE, Schue TJ (1996) Galvanic cathodic protection of reinforced concrete bridge members using sacrificial anodes attached by conductive adhesives
93. Ahmad S, Basavaraja LR, Bhattacharjee B (2000) Design procedures for cathodic protection systems for RC members. Indian Concr J 74:208–213
94. Liu YJ, Shi XM (2009) Electrochemical chloride extraction and electrochemical injection of corrosion inhibitor in concrete: state of the knowledge. Corros Rev 27:53–81
95. Baldenebro Lopez FJ, Barrios Durstewitz CP, Fajardo San Miguel G, Nuñez Jaquez RE, Almeraya Calderon F, Almaral-Sánchez JL, Castorena Gonzalez JH (2010) Electrochemical realkalisation of reinforced concrete using a conductive mortar anode. ECS Trans 29:125–131
96. Marcotte TD, Hansson CM, Hope BB (1999) The effect of the electrochemical chloride extraction treatment on steel-reinforced mortar Part I: electrochemical measurements. Cem Concr Res 29:1555–1560
97. Saraswathy V, Lee HS, Karthick S, Kwon SJ (2018) Extraction of chloride from chloride contaminated concrete through electrochemical method using different anodes. Constr Build Mater 158:549–562
98. Elsener B, Angst U (2007) Mechanism of electrochemical chloride removal. Corros Sci 49:4504–4522
99. Page CL (2000) Repair of corroded reinforcement in concrete using sacrificial anodes. US Pat 6(022):469
100. Siegwart M, Lyness JF, McFarland BJ (2003) Change of pore size in concrete due to electrochemical chloride extraction and possible implications for the migration of ions. Cem Concr Res 33:1211–1221
101. Yeih W, Chang JJ, Hung CC (2006) Selecting an adequate procedure for the electrochemical chloride removal. Cem Concr Res 36:562–570
102. Angst U, Elsener B, Larsen CK, Vennesland Ø (2009) Critical chloride content in reinforced concrete—a review. Cem Concr Res 39:1122–1138
103. Orellan JC, Escadeillas G, Arliguie G (2004) Electrochemical chloride extraction: efficiency and side effects. Cem Concr Res 34:227–234
104. Sánchez MJ, Garcés P, Climent MA (2006) Electrochemical extraction of chlorides from reinforced concrete: variables affecting treatment efficiency. Mater Construcción 56:17–26
105. de Almeida Souza L R, de Medeiros MHF, Pereira E, Capraro APB (2017) Electrochemical chloride extraction: efficiency and impact on concrete containing 1% of NaCl. Constr Build Mater 145:435–444
106. Callaghan BG (1993) The performance of a 12% chromium steel in concrete in severe marine environments. Corros Sci 35:1535–1541
107. Pyc WA, Weyers RE, Sprinkel MM (1998) Corrosion protection performance of corrosion inhibitors and epoxy-coated reinforcing steel in a simulated concrete pore water solution (Virginia)
108. Rasheeduzzafar Dakhil FH, Bader MA, Khan MM (1992) Performance of corrosion-resisting steels in chloride-bearing concrete. ACI Mater J 89:439–448
109. Vedalakshmi R, Kumar K, Raju V, Rengaswamy NS (2000) Effect of prior damage on the performance of cement based coatings on rebar: macrocell corrosion studies. Cem Concr Compos 22:417–421
110. Rengaswamy NS, Srinivasan S, Balasubramanian TM (1988) Inhibited and sealed cement slurry coating of steel rebar—a state of art report. Trans SAEST 23:163–173
111. Thangavel K, Rengaswamy NS, Balakrishnan K (1995) Influence of protective coatings on steel-concrete bond. Indian Concr J 69:191–196
112. Hou J, Fu X, Chung DDL (1997) Improving both bond strength and corrosion resistance of steel rebar in concrete by water immersion or sand blasting of rebar. Cem Concr Res 27:679–684
113. Fu X, Chung DDL (1996) Improving the bond strength between steel rebar and concrete by oxidation treatments of the rebar. Cem Concr Res 26:1499–1503
114. Song H-W, Lee C-H, Ann KY (2008) Factors influencing chloride transport in concrete structures exposed to marine environments. Cem Concr Compos 30:113–121
115. de Vries IJ, Polder RB (1997) Hydrophobic treatment of concrete. Constr Build Mater 11:259–265
116. Delucchi M, Barbucci A, Cerisola G (1997) Study of the physicochemical properties of organic coatings for concrete degradation control. Constr Build Mater 11:365–371
117. Franzoni E, Pigino B, Pistolesi C (2013) Ethyl silicate for surface protection of concrete: performance in comparison with other inorganic surface treatments. Cem Concr Compos 44:69–76
118. Pan X, Shi Z, Shi C, Ling TC, Li N (2017) A review on concrete surface treatment Part I: types and mechanisms. Constr Build Mater 132:578–590
119. Diamanti MV, Brenna A, Bolzoni F, Berra M, Pastore T, Ormellese M (2013) Effect of polymer modified cementitious coatings on water and chloride permeability in concrete. Constr Build Mater 49:720–728
120. Bertolini L, Elsener B, Pedeferri P, Redaelli E, Polder R (2013) Corrosion of steel in concrete : prevention, diagnosis, repair. Wiley, Hoboken
121. Batis G, Pantazopoulou P, Routoulas A (2003) Corrosion protection investigation of reinforcement by inorganic coating in the presence of alkanolamine-based inhibitor. Cem Concr Compos 25:371–377
122. Johnson K, Schultz AE, French C (2009) Crack and concrete deck sealant performance 89261
123. McGettigan E (1995) Factors affecting the selection of water-repellent treatments. APT Bull. 26:22–26
124. Woo RSC, Zhu H, Chow MMK, Leung CKY, Kim J-K (2008) Barrier performance of silane–clay nanocomposite coatings on concrete structure. Compos Sci Technol 68:2828–2836
125. Dai J-G, Akira Y, Wittmann FH, Yokota H, Zhang P (2010) Water repellent surface impregnation for extension of service life of reinforced concrete structures in marine environments: the role of cracks. Cem Concr Compos 32:101–109
126. Jiang L, Xue X, Zhang W, Yang J, Zhang H, Li Y, Zhang R, Zhang Z, Xu L, Qu J, Song J, Qin J (2015) The investigation of factors affecting the water impermeability of inorganic sodium silicate-based concrete sealers. Constr Build Mater 93:729–736
127. Sandrolini F, Franzoni E, Pigino B (2012) Ethyl silicate for surface treatment of concrete—Part I: pozzolanic effect of ethyl silicate. Cem Concr Compos 34:306–312
128. Russo GM, Simon GP, Incarnato L (2006) Correlation between rheological, mechanical, and barrier properties in new copolyamide-based nanocomposite films. Macromolecules 39:3855–3864
129. Basheer L, Kropp J, Cleland DJ (2001) Assessment of the durability of concrete from its permeation properties: a review. Constr Build Mater 15:93–103
130. Papadakis VG (2000) Effect of supplementary cementing materials on concrete resistance against carbonation and chloride ingress. Cem Concr Res 30:291–299
131. Ha TH, Muralidharan S, Bae JH, Ha YC, Lee HG, Park KW, Kim DK (2007) Accelerated short-term techniques to evaluate the corrosion performance of steel in fly ash blended concrete. Build Environ 42:78–85

132. Boa AR, Topu LB (2012) Influence of fly ash on corrosion resistance and chloride ion permeability of concrete. Constr Build Mater 31:258–264
133. Chindaprasirt P, Chotithanorm C, Cao HT, Sirivivatnanon V (2007) Influence of fly ash fineness on the chloride penetration of concrete. Constr Build Mater 21:356–361
134. Güneyisi E, Özturan T, Gesoğlu M (2005) A study on reinforcement corrosion and related properties of plain and blended cement concretes under different curing conditions. Cem Concr Compos 27:449–461
135. Holland RB, Kurtis KE, Kahn LF (2016) Effect of different concrete materials on the corrosion of the embedded reinforcing steel. Corros Steel Concr Struct (Elsevier), pp 131–47
136. Cabrera JG, Claisse PA (1999) Oxygen and water vapour transport in cement-silica fume pastes. Constr Build Mater 13:405–414
137. Bentz DP (2000) Influence of silica fume on diffusivity in cement-based materials II. Multi-scale modeling of concrete diffusivity. Cem Concr Res 30:1121–1129
138. Farahani A, Taghaddos H, Shekarchi M (2015) Prediction of long-term chloride diffusion in silica fume concrete in a marine environment. Cem Concr Compos 59:10–17
139. Bentz DP, Jensen OM, Coats AM, Glasser FP (2000) Influence of silica fume on diffusivity in cement-based materials I. Experimental and computer modeling studies on cement pastes. Cem Concr Res 30:953–962
140. Jung MS, Kim KB, Lee SA, Ann KY (2018) Risk of chloride-induced corrosion of steel in SF concrete exposed to a chloride-bearing environment. Constr Build Mater 166:413–422
141. Cabrera JG, Claisse PA, Hunt DN (1995) A statistical analysis of the factors which contribute to the corrosion of steel in Portland cement and silica fume concrete. Constr Build Mater 9:105–113
142. Heniegal AM, Amin M, Youssef H (2017) Effect of silica fume and steel slag coarse aggregate on the corrosion resistance of steel bars. Constr Build Mater 155:846–851
143. Muhmood L, Vitta S, Venkateswaran D (2009) Cementitious and pozzolanic behavior of electric arc furnace steel slags. Cem Concr Res 39:102–109
144. Taylor R, Richardson IG, Brydson RMD (2010) Composition and microstructure of 20-year-old ordinary Portland cement-ground granulated blast-furnace slag blends containing 0 to 100% slag. Cem Concr Res 40:971–983
145. Teng S, Lim TYD, Sabet Divsholi B (2013) Durability and mechanical properties of high strength concrete incorporating ultra fine ground granulated blast-furnace slag. Constr Build Mater 40:875–881
146. Thomas MDA, Bamforth PB (1999) Modeling chloride diffusion in concrete effect of fly ash and slag. Cem Concr Res 29:487–495
147. Topcu IB, Boga AR (2010) Effect of ground granulate blast-furnace slag on corrosion performance of steel embedded in concrete. Mater Des 31:3358–3365
148. Siddique R, Klaus J (2009) Influence of metakaolin on the properties of mortar and concrete: a review. Appl Clay Sci 43:392–400
149. Batis G, Pantazopoulou P, Tsivilis S, Badogiannis E (2005) The effect of metakaolin on the corrosion behavior of cement mortars. Cem Concr Compos 27:125–130
150. Barbhuiya S, Chow P, Memon S (2015) Microstructure, hydration and nanomechanical properties of concrete containing metakaolin. Constr Build Mater 95:696–702
151. Gruber KA, Ramlochan T, Boddy A, Hooton RD, Thomas MDA (2001) Increasing concrete durability with high-reactivity metakaolin. Cem Concr Compos 23:479–484
152. Keleştemur O, Demirel B (2015) Effect of metakaolin on the corrosion resistance of structural lightweight concrete. Constr Build Mater 81:172–178
153. Kannan V, Ganesan K (2014) Chloride and chemical resistance of self compacting concrete containing rice husk ash and metakaolin. Constr Build Mater 51:225–234
154. Daniyal M, Azam A, Akhtar S (2018) Application of nanomaterials in civil engineering advanced structured materials, vol 84. Springer Nature Singapore Pvt Ltd., Singapore, pp 169–189
155. Anon (2015) ISO 8044:2015, Corrosion of metals and alloys—basic terms and definitions. Int. Organ. Stand. 24
156. Nathan CC (1973) Corrosion inhibitors. Natl Assoc Corros, Eng, p 279
157. ACI Committee 116 (1985) ACI 116R-85, Cement and Concrete Terminology (Michigan)
158. Hope BB, Ip AKC (1987) The research and development branch, Report No. ME-87-09, Ontario Ministry of Transportation (Ontario)
159. Hansson CM, Mammoliti L, Hope BB (1998) Corrosion inhibitors in concrete—part I: the principles. Cem Concr Res 28:1775–1781
160. Roberge P (1995) Corrosion inhibitors handbook of corrosion engineering pp 833–62
161. Söylev TA, Richardson MG (2008) Corrosion inhibitors for steel in concrete: state-of-the-art report. Constr Build Mater 22:609–622